Risø–R–766(EN)

Cups, Props and Vanes

Leif Kristensen

Risø National Laboratory, Roskilde, Denmark
August 1994

Abstract We discuss the dynamics of the cup anemometer, the propeller anemometer and the wind vane. The phenomenological model by Kristensen (1993) is modified to describe the motion of the propeller anemometer. We use the well-know second-order differential equation describing the motion of the wind vane to study the properties of the vane itself and the vane in combination with a cup and a vane. It is argued that even the simplest question about how to record the signal from a cup anemometer has an ambiguous answer and can lead to a, not necessarily small, systematic error in the measured mean wind speed. We show how it is possible to measure the entire wind direction variance by utilizing the fact that an underdamped vane by 'overshooting' may compensate for the high-frequency variance loss if the damping coefficient is about 0.4. Finally we discuss possible sources of bias on the measured mean-wind speed when using a propeller-vane anemometer. It turns out that this anemometer has the same type biases from the lateral and vertical wind fluctuations as has the cup anemometer. In addition there are bias contributions from misalignment between the mean wind and the propeller axis and from the translatory motion of the propeller itself with respect to the vertical wind-vane axis.

ISBN 87–550–2006–2
ISSN 0106–2840

Information Service Department · Risø · 1994

Contents

1 Introduction

Probably the most common anemometers are the rotating anemometers, cups and propellers, and the Pitot tube. They are often used together with a wind vane for wind-direction determination. Such a combination is a sturdy and reliable instrument package for the determination of the mean of the horizontal wind-velocity component. It is easy to operate and is used in weather stations, airports, wind farms and sites where large structures such as bridges are under construction. (The Pitot tube without wind vane is standard instrumentation in aircraft for measuring airspeed.)

As indicated in the title, we are here concerned only with the rotating anemometers and the wind vane. There is a vast amount of literature about these instruments. Wyngaard (1981) has given a very well written summary and also provided a comprehensive list of useful references. There are two major reasons why so much has been written about the cup anemometer, which was invented as early as 1846 by the Irish astronomer Thomas Romney Robinson (Middleton, 1969 and Wyngaard, 1981) and which, in almost the same standard design, is still in use. One is the remarkable linearity of the calibration, the other the so-called *overspeeding* which, allegedly, should cause large systematic errors when trying determine of the mean wind speed in more than light turbulence. Kristensen (1993) discussed this overspeeding in much detail and developed a phenomenological model for the forcing of the cup-anemometer rotor. Here we limit ourselves to a short description of this model and the experimental justification for it and to a discussion of the proper signal processing with and without a wind-vane signal.

It is postulated that the forcing model for the cup anemometer with a slight modification can be applied to a propeller. The vane alone and the propeller vane will be discussed in great detail in order to specify, as in the case of the cup anemometer, what kind of systematic errors must be expected when measuring the mean wind speed.

2 The Cup Anemometer

Figure 1 shows a cup anemometer with three cups. As a field instrument and general-purpose anemometer for operational purposes the cup anemometer has at least two good properties. It is omnidirectional; when mounting the instrument, it is only necessary to make sure that the axis is pointing in the vertical direction. Further, the cup anemometer is robust and easy to operate.

We assume that the cup anemometer is mounted with its axis vertical. In this case the equation for the rotation rate of the rotor can be written

$$\dot{\tilde{s}} = F(\tilde{s}, \sqrt{\tilde{u}^2 + \tilde{v}^2}, \tilde{w}), \tag{1}$$

where $\tilde{u}$, $\tilde{v}$ and $\tilde{w}$ are the instantaneous horizontal and vertical wind components and $\tilde{s}$ is the instantaneous rotation rate of the anemometer rotor in rad s^{-1}. The angular momentum of the rotor is proportional to $\tilde{s}$ and (1) just states that the rate of change of the angular momentum is equal to the torque on the rotor. This torque is caused by the wind and the friction in the instrument bearings. For a

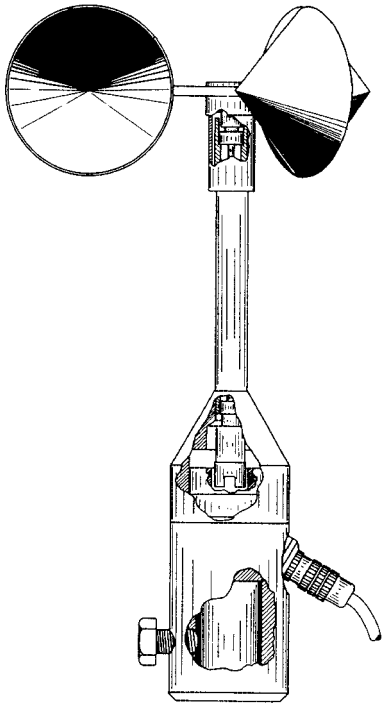

Figure 1. The Risø cup anemometer. The height is 0.26 m.

real cup anemometer the right-hand side, the torque divided by the moment of inertia, is a function of $\tilde{s}$, the total horizontal wind component $\tilde{h} = \sqrt{\tilde{u}^2 + \tilde{v}^2}$ as well as the vertical wind component $\tilde{w}$.

2.1 Phenomenological Model

It was shown by Kristensen (1993) that we can explain behaviour of the cup anemometer by assuming that the function F has the form

$$F(\tilde{s}, \tilde{h}, \tilde{w}) = \frac{(\tilde{h} + \mu_1\tilde{w} - \ell\tilde{s})(\tilde{h} + \mu_1\tilde{w} + \Lambda\tilde{s})}{\ell_0(\ell + \Lambda)} + \frac{\mu_2\tilde{w}^2}{2\ell_0\ell}. \tag{2}$$

Here ℓ, ℓ_0, Λ, μ_1 and μ_2 are instrument constants, the first three with the dimension of length and the last two dimensionless. The first quantity ℓ is the *calibration distance* which, under conditions with constant magnitude U of the horizontal wind velocity, can be interpreted as the length of the column of air which has to pass through the anemometer for the cup rotor to turn one radian. The second quantity ℓ_0 is the so-called *distance constant* which is the length of the column of air which has to pass through the anemometer before it has reacted with $1-\exp(-1) \approx 0.63$ of its final response to a sudden change in the wind speed. The last instrument length scale Λ cannot be interpreted as directly as ℓ and ℓ_0. Finally, the constants μ_1 and μ_2 characterize the *angular response* of the cup anemometer up to second order in the angle between the direction of the wind vector and the rotor plane; if they are both zero this response is a *cosine response*, which means that the anemometer is insensitive to the vertical wind component. It is interesting that if we can construct an anemometer with $\Lambda = \ell$, $\mu_1 = 0$ and $\mu_2 = 1$ this instrument

will be responding only to the magnitude of the *three-dimensional* velocity vector since

$$F(\tilde{s}, \tilde{h}, \tilde{w}) = \frac{\tilde{u}^2 + \tilde{v}^2 + \tilde{w}^2 - \ell^2 \tilde{s}^2}{2\ell\ell_0}. \tag{3}$$

Equations (1) and (2) imply that the steady-state calibration of the cup anemometer is linear without offset. This is easily seen by setting $\dot{\tilde{s}}$ and $\tilde{w}$ equal to zero and solving for $S = \tilde{s}$. The result is

$$S = \frac{U}{\ell}. \tag{4}$$

Experience actually shows that the calibration is indeed approximately linear with an offset U_0 which in most cases can be ignored when the wind speed is more than a few meters per second*. Brazier (1914) and Patterson (1926) demonstrated that the linearity is better the shorter the diameter of the cup rotor. Patterson (1926) determined, for a number of cup anemometers, the *anemometer factor*, defined as

$$f = \frac{U}{rS} = \frac{\ell}{r}, \tag{5}$$

where r is the cup radius, i.e. the distance from the axis to the center of one of the cups. He found that, depending on cup diameter and r, the anemometer factor varies between 2.5 and 3.5. We expect ℓ and Λ to be dependent on only the anemometer geometry and independent of the mass and mass distribution of the cup rotor. For the Risø cup anemometer shown in Figure 1, $\ell = 20$ cm and $r = 6$ cm. Correspondingly, $f = 3.3$.

The distance constant depends on the moment of inertia I, i.e. of the cup-rotor mass distribution, and is given by

$$\ell_0 = \frac{2I}{\rho C A r(\ell + \Lambda)}, \tag{6}$$

where C is a dimensionless constant of order unity, $\rho \approx 0.0013$ g cm^{-3} the density of air and A an effective cup area.

Since I is proportional to the rotor density ρ_r and to the fifth power of its linear dimensions ($\propto r$) we conclude from (6) that for geometrically similar rotors ($A \propto r^2$) the distance constant is proportional to ρ_r/ρ and to r. The rotor of the Risø model (Busch *et al.*, 1980) in Figure 1 is made of carbon reinforced plastic with a density ρ_r of about 1.5 g cm^{-3}. The distance constant ℓ_0 was determined in wind-tunnel studies to be 170 cm. This is a rather modern and sturdy cup anemometer, which is used for routine measurements of mean wind speed by Risø National Laboratory. Older models are typically made of steel and they are often larger, with radii of about 15 cm. They have distance constants of about 20 m and reacts consequently much slower than newer models of standard cup anemometers.

2.2 Anemometer Dynamics

When exposed to the fluctuating, turbulent wind the first-order response of a cup anemometer is that of a first-order filter. Assuming that the mean of the vertical

*If the offset must be taken into account this is done by replacing, in (2), $\tilde{h}$ by $\tilde{h} - U_0$. Then the calibration expression (4) becomes $S = (U - U_0)/\ell$.

velocity component is zero and that the coordinate system is chosen such that the lateral velocity component $\tilde{v}$ also has a zero mean, we may decompose the instantaneous wind vector and the anemometer response according to

$$\left\{ \begin{array}{l} \tilde{u} \\ \tilde{v} \\ \tilde{w} \\ \tilde{s} \end{array} \right\} = \left\{ \begin{array}{l} U+u \\ v \\ w \\ S+s \end{array} \right\}. \tag{7}$$

Kristensen (1993) has shown that first-order perturbation applied to (1) with F given by (2) leads to

$$\dot{s} + \frac{s}{\tau_0} = \frac{1}{\ell} \left\{ \frac{u}{\tau_0} + \mu_1 \frac{w}{\tau_0} \right\}, \tag{8}$$

where

$$\tau_0 = \frac{\ell_0}{U}. \tag{9}$$

Equation (8) is the equation for a first-order, linear filter with the time constant τ_0 which, as (9) shows, is inversely proportional to the magnitude of mean-wind velocity.

The properties of this filter can by studied in a number of ways. One simple and illuminating diagnostic tool is a study of its response to a step function given by

$$u(t) = \left\{ \begin{array}{ll} 0 & \text{for } t < 0 \\ \Delta U & \text{for } t \geq 0 \end{array} \right. \tag{10}$$

with $w(t) = \tilde{w}$ kept equal to zero.

In this case, the response will be

$$s(t) = \frac{\Delta U}{\ell}(1 - \mathrm{e}^{-t/\tau_0}) \tag{11}$$

—the classical response of a first-order system to a step function. Figure 2 shows how the response adjusts to the new equilibrium value of the input. It grows such that when $t = \tau_0$ it has attained $\approx 63\%$ of its terminal value $s(\infty)$.

Applying Taylor's hypothesis (for 'frozen turbulence'), we may convert the temporal variable to a spatial variable in the direction x of the mean wind by

$$x = U \times t \tag{12}$$

in which case (8) takes the form

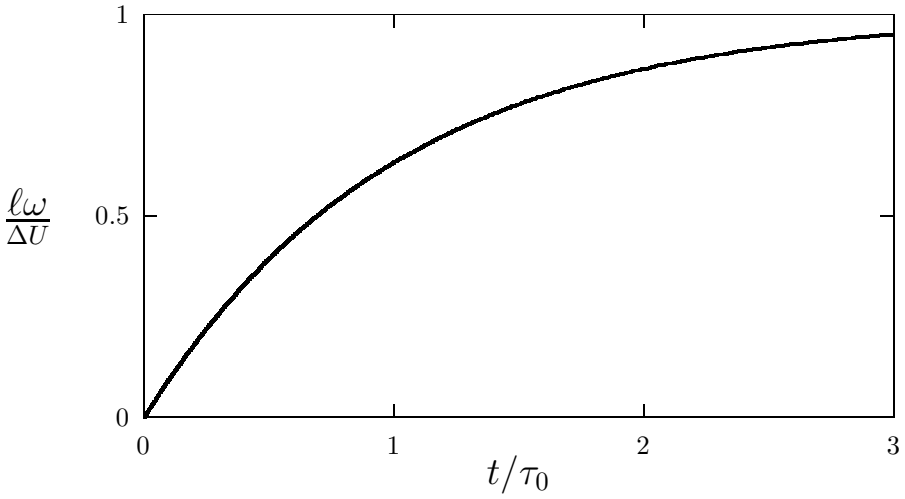

Figure 2. First-order response (11) of a cup anemometer to a step input ΔU.

$$\frac{ds}{dx} + \frac{s}{\ell_0} = \frac{1}{\ell}\left\{\frac{u}{\ell_0} + \mu_1\frac{w}{\ell_0}\right\}. \tag{13}$$

In (13) the coefficients are all instrument constants, independent of the wind speed U. The implication is that the cup anemometer is a spatial rather than an temporal filter. This is fortunate because atmospheric turbulence in most cases, i.e. when the mean wind is large compared to the r.m.s. fluctuations of the turbulence, can be considered a random, 'frozen' velocity field which is being transported through the observation point by the mean wind.

The first-order perturbation equation (13) is sufficient for applications where we are concerned with spectral filtering of the velocity signal. However, if we want to quantify a phenomenon as overspeeding we will need to derive a second-order perturbation equation, as shown in Kristensen (1993).

Following Wyngaard *et al.* (1974), we write this equation in the dimensionless form

$$\begin{aligned}\ell_0\frac{d}{dx}\left(\frac{s}{S}\right) + \frac{s}{S} \quad = \quad & a_1\frac{u}{U} + a_2\frac{w}{U} \\ & + a_3\left(\frac{s}{S}\right)^2 + a_4\left(\frac{u}{U}\right)^2 + a_5\left(\frac{w}{U}\right)^2 \\ & + a_6\left(\frac{s}{S}\right)\left(\frac{u}{U}\right) + a_7\left(\frac{u}{U}\right)\left(\frac{w}{U}\right) + a_8\left(\frac{w}{U}\right)\left(\frac{s}{U}\right). \end{aligned} \tag{14}$$

Wyngaard *et al.* (1974) now determined experimentally the eight coefficients $a_1, \ldots, a_8$ in a wind tunnel for a particular cup anemometer. They did that by measuring the torque $I \times F(S + s, U + u, w)$ when the anemometer rotor, by means of a small electric motor, was brought into a steady rotation with a rate independent of the wind speed in the tunnel. In this way they could determine the function F in a range of the independent perturbation variables s, u and w. The

way the measurements were set up they were not able to vary the lateral velocity component $\tilde{v}$.

They found

$$\left\{\begin{array}{c} a_1 \\ a_2 \\ a_3 \\ a_4 \\ a_5 \\ a_6 \\ a_7 \\ a_8 \end{array}\right\} = \left\{\begin{array}{rr} 1.03 & < \pm 10\% \\ 0.06 & \pm 0.1 \\ -0.23 & < \pm 10\% \\ 0.96 & < \pm 10\% \\ 0.67 & \pm 0.1 \\ -0.73 & < \pm 10\% \\ 0.04 & \pm 0.1 \\ -0.12 & \pm 0.1 \end{array}\right\}. \tag{15}$$

Applying (2), we may also write the second-order perturbation equation as

$$\begin{aligned} \ell_0 \frac{d}{dx}\left(\frac{s}{S}\right) + \frac{s}{S} \quad = \quad & \frac{u}{U} + \mu_1 \frac{w}{U} \\ & - \frac{\Lambda}{\ell+\Lambda}\left(\frac{s}{S}\right)^2 + \frac{\ell}{\ell+\Lambda}\left(\frac{u}{U}\right)^2 \\ & + \frac{1}{2}\left(\frac{v}{U}\right)^2 + \left\{\frac{\mu_1^2 \ell}{\ell+\Lambda} + \frac{\mu_2}{2}\right\}\left(\frac{w}{U}\right)^2 \\ & - \frac{\ell-\Lambda}{\ell+\Lambda}\left(\frac{s}{S}\right)\left(\frac{u}{U}\right) + \frac{2\mu_1 \ell}{\ell+\Lambda}\left(\frac{u}{U}\right)\left(\frac{w}{U}\right) \\ & - \mu_1 \frac{\ell-\Lambda}{\ell+\Lambda}\left(\frac{w}{U}\right)\left(\frac{s}{U}\right), \end{aligned} \tag{16}$$

where we have assumed a calibration of the form (4).

Comparing (14) and (16), we see that there are the following constraints

$$a_1 = 1, \tag{17}$$

$$a_3 + a_4 + a_6 = 0, \tag{18}$$

$$a_2 - a_7 - a_8 = 0 \tag{19}$$

and

$$2a_3 + a_6 + 1 = 0. \tag{20}$$

We see that the data (15) are consistent with these four relations[†].

Coppin (1982) carried out a similar investigation on seven different cup anemometers. Only a_1, a_3, a_3, a_5 and a_6 were determined in this investigation. The results are shown in tabular form together with the result by Wyngaard *et al.* (1974).

Type	a_1	a_3	a_4	a_5	a_6
Friedrichs	1.27	0.00	1.10	0.85	−1.17
Siggelkow	1.18	−0.05	1.03	0.90	−0.90
Teledyne 3	1.25	−0.19	1.11	0.82	−0.86
Teledyne 6	1.26	−0.20	1.15	0.47	−0.89
Gill 3	1.22	−0.20	1.14	≈ 0	−0.79
Casella	1.19	−0.29	0.98	≈ 0	−0.69
Thies	1.18	−0.11	1.18	0.95	−1.26
Wyngaard	1.03	−0.23	0.96	0.67	−0.73

As the accuracy of the measurements is not stated explicitly in the 1982 investigation by Coppin it is not possible to judge if the relations (17), (18), (19) and (20) are consistent with the measurements. It is claimed though that (18) is satisfied within the experimental accuracy in all seven cases.

It is interesting to note that no positive values of a_3 were found. We assume that this is generally true for all cup anemometers and, since $a_3 = -\Lambda/(\ell + \Lambda)$, the implication is that Λ is never negative for a cup anemometer. This in turn means that the equation $F(S, U, 0) = 0$ has only one root for which $U/S = \ell$ is positive[‡].

2.3 Mean Wind-Speed Measurements

The automatic recording of the cup anemometer signal can be done in many ways. We must realize, however, that even if the wind speed is constant, the angular velocity $\tilde{s}$ of the rotor varies over one full rotation. This means that the rotation rate must be averaged over a least on full revolution before recording and interpretation. If it takes the time Δt for the cup rotor to complete one full revolution, the average wind speed in this period is $2\pi\ell/\Delta t$. When determining the average wind speed U over the period T we simply calculate $N \times 2\pi\ell/T$, where N is the number of revolutions of the rotor in the period T. Roughly stated, this corresponds to the displacement $N \times 2\pi\ell$ of an air particle in the period of time T. It is quite easy to build an electronic system which gives an electric pulse for every rotor revolution and then it is just a matter of counting how many pulses there are in the period T.

[†]Combining (19) and (20), we see that $a_2(2a_3+a_6)+a_7+a_8 = 0$. In Kristensen (1993) there is an unfortunate mistake in the corresponding equation (51) which reads $2a_2(a_3+a_6)+a_7+a_8 = 0$.

[‡]The requirement that there could be only one steady-state calibration expression for a cup anemometer was used by Kristensen (1993) as a proof that Λ must be positive. Of course this argument is incorrect as the phenomenological model (2) is assumed valid and applied only close to a steady state where $(\tilde{s}, \tilde{h})$ is close to (S, U).

Let us for a moment consider what this means. The average wind speed U_i during the ith revolution is $2\pi\ell/\Delta t_i$, where Δt_i is the time it takes for the rotor to perform the ith revolution. According to the definition of U, we have

$$U = \frac{N2\pi\ell}{T} = \frac{N2\pi\ell}{\sum_{i=1}^{N}\Delta t_i} = \left\{\frac{1}{N}\sum_{i=1}^{N}\frac{1}{U_i}\right\}^{-1}. \tag{21}$$

We could imagine another procedure. We could determine, also by simple means, the duration Δt_i of each revolution and then calculate the average of all values of $U_i = 2\pi\ell/\Delta t_i$ according to the equation

$$\widehat{U} = \frac{1}{N}\sum_{i=1}^{N}U_i. \tag{22}$$

We note that

$$\widehat{U} \geq U, \tag{23}$$

where equality holds when all the U_i's are the same, i.e. if the wind speed is constant. To see this, we study the ratio

$$\frac{\widehat{U}}{U} \equiv \frac{1}{N^2}\sum_{i=1}^{N}U_i\sum_{j=1}^{N}U_j^{-1} = \frac{1}{2N^2}\sum_{i=1}^{N}\sum_{j=1}^{N}\left\{\frac{U_i}{U_j}+\frac{U_j}{U_i}\right\}. \tag{24}$$

Now, let

$$x = \frac{U_i}{U_j} \tag{25}$$

and

$$f(x) = x + \frac{1}{x}. \tag{26}$$

We see immediately by differentiation of $f(x)$ that this function has one minimum at 2 for $x = 1$, corresponding to $U_i = U_j$. Using this in (24), we conclude

$$\frac{\widehat{U}}{U} \geq \frac{1}{2N^2}\sum_{i=1}^{N}\sum_{j=1}^{N}2 = 1. \tag{27}$$

Exactly by how much $\widehat{U}$ is an overestimation depends primarily on how much U_i varies with i. It can quite easily be shown that in the limit $N \to \infty$ we have

$$\widehat{U} \approx U\left\{1+\frac{\sigma_U^2}{U^2}\right\}, \tag{28}$$

where σ_U^2 is the variance of all the measured U_i's.

Later we will discuss how to operate a cup anemometer together with a wind vane to obtain mean value and direction of the horizontal wind vector.

3 The Propeller Anemometer

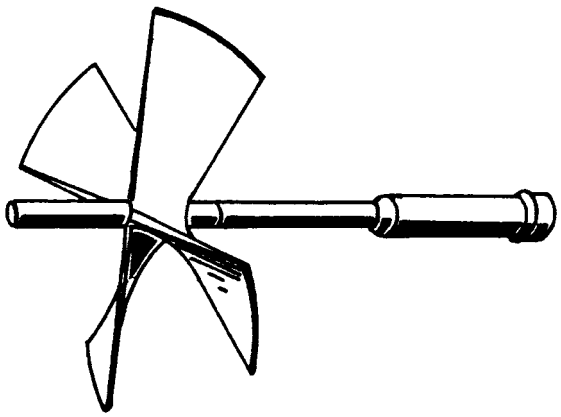

Figure 3. Gill Propeller. The rotor diameter is 0.19 m. [From Busch et al. *(1980)]*

Figure 3 shows a Gill propeller. We consider a coordinate system with the mean wind vector $\boldsymbol{U}$ in the direction of the propeller axis. The equation of motion is then

$$\dot{\tilde{s}} = F(\tilde{s}, \tilde{u}, \sqrt{\tilde{v}^2 + \tilde{w}^2}), \tag{29}$$

where $\tilde{u}$, $\tilde{v}$ and $\tilde{w}$ are the instantaneous horizontal and vertical wind components and $\tilde{s}$ is the instantaneous rotation rate of the anemometer rotor in rad s^{-1}. The angular momentum of the rotor is proportional to $\tilde{s}$ and (29) just states that the rate of change of the angular momentum is equal to the torque on the rotor. This torque is caused by the wind and the friction in the instrument bearings.

We assume that the dynamics of the propeller can be described by the same equation as that pertaining to a cup anemometer and given by Kristensen (1993), except that the dependence of the lateral wind component is the same as the dependence of the vertical wind component, that the angular response is symmetric and that there is no u-bias. This last requirement implies according to Kristensen (1993) that $\Lambda = \infty$ in (2) so that

$$F(\tilde{s}, \tilde{u}, \sqrt{\tilde{v}^2 + \tilde{w}^2}) = \frac{\{\tilde{u} - \ell\tilde{s}\}\tilde{s}}{\ell_0} + \mu_2 \frac{\tilde{v}^2 + \tilde{w}^2}{2\ell\ell_0}. \tag{30}$$

Here ℓ is the calibration distance, ℓ_0 the distance constant and μ_2 a measure of the sensitivity to the wind component perpendicular to the propeller axis. This

last quantity can be defined in terms the angular response function $\mathcal{G}(\vartheta)$ (see Kristensen (1993)), where ϑ is the angle between the wind velocity and the propeller axis.

$$\mathcal{G}(\vartheta) = \cos(\vartheta) + \frac{\mu_2}{2}\vartheta^2 \tag{31}$$

and we note that $\mu_2 = 0$ corresponds to a *cosine response*.

When $\tilde{u}$ is constant and equal to U while $\tilde{v} = \tilde{w} = 0$, we obtain after some time $\dot{\tilde{s}} = 0$, i.e. $\tilde{s}$ becomes constant. Denoting this constant rotation rate S, the steady-state calibration is obtained, as in the case of the cup anemometer, by solving

$$F(S, U, 0) = 0. \tag{32}$$

The model (30) implies that S and U are proportional and related by

$$U = \ell S. \tag{33}$$

According to Busch *et al.* (1980) the calibration is linear. Here we also assume that there is proportionality between U and S.

4 The Wind Vane

In order to avoid future confusion we will first specify the definition of the wind direction.

According to the traditions in operational meteorology, the mean wind direction D is defined as the direction from where the wind comes. In other words, the wind direction is, according to this definition, the direction you are looking into, when the wind is blowing in your face. If the wind blows from north then $D = 0°$ and D is measured clockwise so that east corresponds to $D = 90°$, south to $D = 180°$ and west to $D = 270°$.

In physical meteorology we often work with a wind direction $\tilde{\alpha}$ which is the direction of the mean wind velocity vector, i.e. opposite to D. It is measured counterclockwise and usually from east. The relation between D and the mean $\langle\tilde{\alpha}\rangle$ of $\tilde{\alpha}$ is

$$D + \langle\tilde{\alpha}\rangle = 270° \tag{34}$$

or, if angles are measured in radians,

$$D + \langle\tilde{\alpha}\rangle = \frac{3}{2}\pi. \tag{35}$$

In short term studies where the wind direction does not change systematically we often chose to set the mean-wind direction equal to zero. We do that here to make the discussion of wind-vane dynamics a little easier.

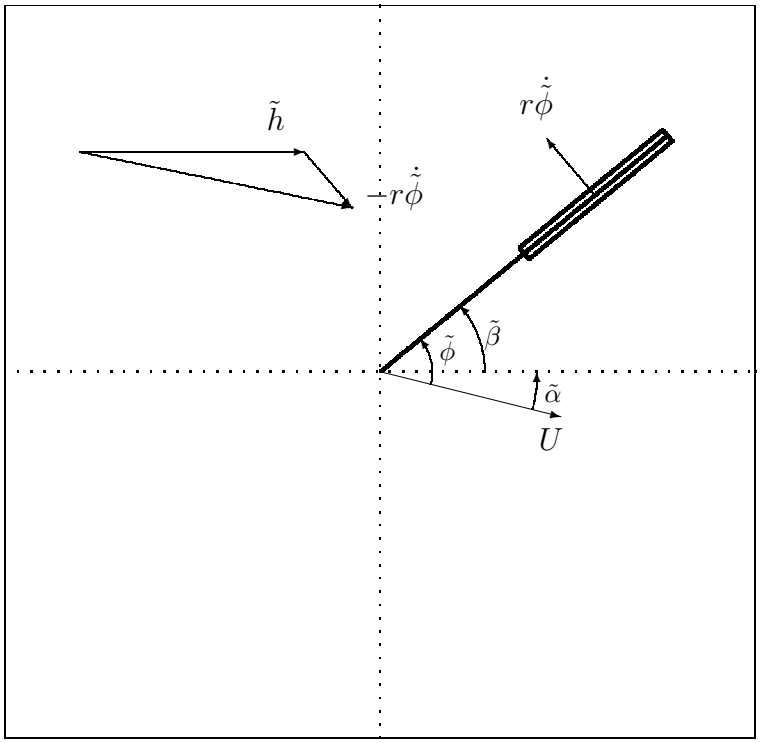

Figure 4. Schematic illustration of the vane motion. Top view.

4.1 Wind-Vane Dynamics

Developing the equation of motion, we restate almost literally the derivation by Larsen and Busch (1974). Figure 4 illustrates the motion of a wind vane. The angle from the mean-wind velocity vector $\boldsymbol{U}$ with magnitude U to the horizontal component of the instantaneous wind-velocity vector with magnitude $\tilde{h}$ is $\tilde{\alpha}$. The angles from this horizontal wind component and from $\boldsymbol{U}$ to the plane of the wind vane are $\tilde{\beta}$ and $\tilde{\phi}$, respectively. The vane is turning with the angular velocity $\dot{\tilde{\phi}}$ with respect to the reference direction given by $\boldsymbol{U}$. This means that the center of mass of the vane is moving horizontally and perpendicular to the vane with the speed $r\dot{\tilde{\phi}}$, where r is the distance from the vane axis to the center of mass. Assuming that all angles are small, it can be shown that the wind force is proportional to the angle $\tilde{\beta}'$ from the instantaneous horizontal wind-velocity component to the *moving* vane. This angle is

$$\tilde{\beta}' = \tilde{\beta} + \frac{r\dot{\tilde{\phi}}}{U}. \tag{36}$$

The equation of motion (for angular momentum) of the vane is

$$I\ddot{\tilde{\phi}} = -r \times \frac{1}{2}\rho U^2 A K \tilde{\beta}', \tag{37}$$

where I is the moment of inertia, A the vane area and K a dimensionless constant. According to the theory for thin aerofoils (see e.g., Batchelor, 1967) K is 2π. Larsen (1986) found $K \approx 1.9$ for his vane. Here we just assume that K is of the order unity.

Substituting (36) in (37) and using the relation

$$\tilde{\phi} = \tilde{\alpha} + \tilde{\beta}, \tag{38}$$

we obtain the second-order differential equation for $\tilde{\phi}$

$$\ddot{\tilde{\phi}} + 2\zeta\omega_0\dot{\tilde{\phi}} + \omega_0^2\tilde{\phi} = \omega_0^2\tilde{\alpha}, \tag{39}$$

where

$$\omega_0 = U\sqrt{\frac{\rho r A K}{2I}} \tag{40}$$

is a characteristic frequency and

$$\zeta = \frac{r}{2}\sqrt{\frac{\rho r A K}{2I}} \tag{41}$$

a positive, dimensionless constant which is independent of U.

We note that

$$\ell_v \equiv \frac{U}{\omega_0} \tag{42}$$

is a characteristic length scale which does not depend on the wind speed. We will call ℓ_v the vane distance constant. Using (42), we may write

$$\zeta = \frac{1}{2}\frac{r}{\ell_v}. \tag{43}$$

Equation (39) describes a so-called damped oscillator with the natural frequency ω_0 and the damping coefficient ζ. The right-hand side, the instantaneous wind direction, is the the input.

As in the case of a first-order, we can study the characteristics of this damped oscillator by looking at its response to a step function.

$$\tilde{\alpha} = \begin{cases} 0 & \text{for } t < 0 \\ \\ \alpha & \text{for } t \geq 0 \end{cases}. \tag{44}$$

The output from (39) is

$$\tilde{\phi}(t) = \alpha \begin{cases} 1 - \exp(-\zeta\omega_0 t)\left\{\cos\left(\sqrt{1-\zeta^2}\,\omega_0 t\right)\right. & \\ \qquad \left. + \dfrac{\zeta}{\sqrt{1-\zeta^2}}\sin\left(\sqrt{1-\zeta^2}\,\omega_0 t\right)\right\}, & 0 \le \zeta < 1 \\ 1 - \exp(-\omega_0 t)\left\{1 + \omega_0 t\right\}, & \zeta = 1 \\ 1 - \exp(-\zeta\omega_0 t)\left\{\cosh\left(\sqrt{\zeta^2-1}\,\omega_0 t\right)\right. & \\ \qquad \left. + \dfrac{\zeta}{\sqrt{\zeta^2-1}}\sinh\left(\sqrt{\zeta^2-1}\,\omega_0 t\right)\right\}, & 1 < \zeta < \infty \end{cases} . \qquad (45)$$

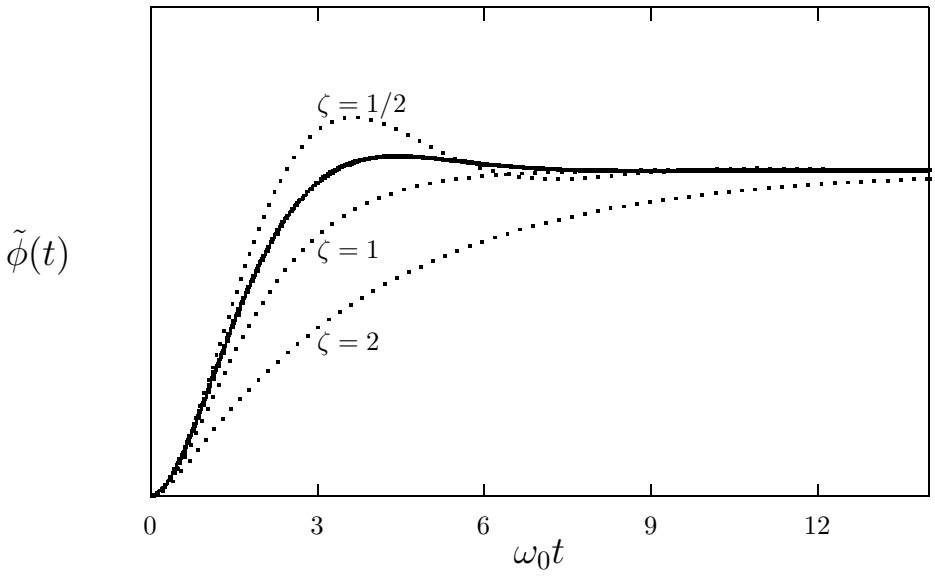

Figure 5. Response of a damped oscillator to a step input.

Figure 5 shows how the response depends on the damping coefficient ζ. When $\zeta \ge 1$ the solution (45) is an increasing function of time whereas it becomes a damped oscillation for $0 < \zeta < 1$. In Figure 5, we we see the response (solid line) $\tilde{\phi}(t)$ with the value $\zeta = 1/\sqrt{2}$. This damping coefficient provides the best compromise between a fast response and minimal 'overshoot'. The vane reacts in this case as a so-called *Butterworth* filter.

In the limit $\zeta \gg 1$ (45) approaches

$$\tilde{\phi}(t) = \alpha\left\{1 - \exp\left(-\frac{\omega_0 t}{2\zeta}\right)\right\}, \qquad (46)$$

which is the response of a first-order filter with the time constant $\tau_0 = 2\zeta/\omega_0$. According to (42) and (43) this time constant can be expressed as

$$\tau_0 = \frac{r}{U} \qquad (47)$$

so that the effective vane distance constant ℓ_{eff} simply becomes equal to $U \times \tau_0 = r$. Figure (6) shows the difference between (45) and (46) when $\zeta = 2$.

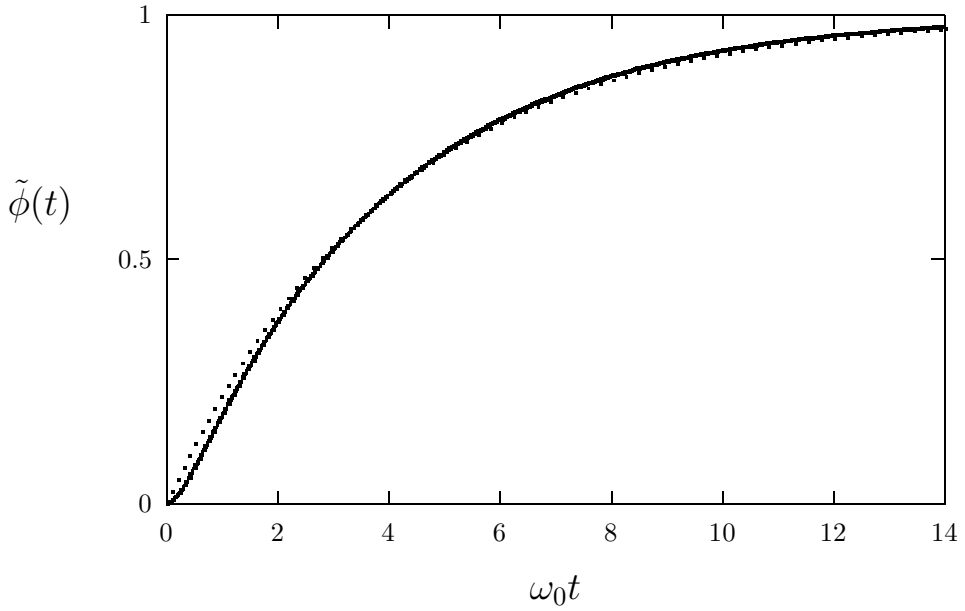

Figure 6. Response of a damped oscillator to a step input for $\zeta = 2$ when $\tilde{\phi}(t)$ is given by (45) (solid line) and by (46) (dotted line).

As discussed in subsection 2.2, the cup anemometer is a genuine first-order filter with a distance constant ℓ_0. If we want to operate the vane together with a cup anemometer it would be best from a theoretical point of view that the vane can also be considered a first-order filter with a distance constant $\ell_{\text{eff}} = r = \ell_0$. Since ℓ_0 is at least about 1 m for a conventional cup anemometer the vane arm r must be rather long. Assuming that the vane is a light (styrofoam) aerofoil with height h and width d, positioned at the end of the vane arm, the main contribution to the moment of inertia I comes from this arm. Denoting the mass per unit length of the arm σ_t, we have

$$I \approx \frac{1}{3}\sigma_t r^3 \tag{48}$$

so that (41) becomes

$$\zeta \approx B\sqrt{\frac{\rho h d}{\sigma_t}}, \tag{49}$$

where B is a dimensionless constant of the order one.

We see that ζ is independent of r. The only ways in which we can increase damping coefficient is therefore by decreasing σ_t of by increasing the area hd of the vane.

The direction sensor described by Larsen and Busch (1974) and by Larsen (1986) has a styrofoam vane with the dimensions $h = 20$ cm, $d = 10$ cm and thickness 0.7 cm. The the arm consisted of two parallel steel tubes of length $(= r + d/2)$ 20 cm and with $\sigma_t = 0.2079$ g cm^{-1}. Inserting in (49) and using $\rho = 0.0013$ g cm^{-3} for the density of air, we obtain $\zeta \sim 1$. It should be possible to construct a wind vane with properties matching those of a cup anemometer.

In some situations as when studying atmospheric dispersion we are more interested in determining the wind direction variance than in matching the filter characteristics of a cup anemometer. Since the wind vane, like the cup anemometer, is by itself a mechanical low-pass filter, a wind direction record will never be able to

show the full contribution to the variance from the high frequencies far beyond U/ℓ_v. However, since the wind-vane filter is of second order, we can take advantage of the fact that an underdamped, second-order filter 'overshoots' at frequencies close to U/ℓ_v so that measured variance around U/ℓ_v compensates for the high-frequency loss. The next subsection is devoted to a discussion of how this might be accomplished by designing a wind vane with a damping coefficient ζ close to 0.4.

4.2 Measuring the Lateral Velocity Variance

Let us start with the dynamic equation for the vane for small direction variations in the deviation $\alpha \equiv \tilde{\alpha} - \langle\tilde{\alpha}\rangle = v/U$ from the mean. Denoting the corresponding vane response ϕ, we rewrite (39) as

$$\ddot{\phi} + 2\zeta\omega_0\dot{\phi} + \omega_0^2\phi = \omega_0^2\frac{v}{U}. \tag{50}$$

Since the distance constant $\ell_v = U/\omega_0$ is constant, it is more practical to operate in the space domain by use of Taylor's hypothesis. The equation of motion (50) is therefore equivalent to

$$\frac{d^2\phi}{dx^2} + \frac{2\zeta}{\ell_v}\frac{d\phi}{dx} + \frac{\phi}{\ell_v^2} = \frac{1}{\ell_v^2}\frac{v}{U}. \tag{51}$$

The measured wind-direction variance $\langle\phi^2\rangle$ is consequently given by

$$\begin{aligned} U^2\langle\phi^2\rangle &= \int_{-\infty}^{\infty}\frac{F_v(k)dk}{(1-\ell_v^2k^2)^2 + 4\zeta^2\ell_v^2k^2} \\ &= \int_{-\infty}^{\infty}F_v(k)dk + \int_{-\infty}^{\infty}\left\{\frac{1}{(1-\ell_v^2k^2)^2 + 4\zeta^2\ell_v^2k^2} - 1\right\}F_v(k)dk \\ &= \langle v^2\rangle + 2\int_0^{\infty}\frac{2(1-2\zeta^2)\ell_v^2k^2 - \ell_v^4k^4}{(1-\ell_v^2k^2)^2 + 4\zeta^2\ell_v^2k^2}F_v(k)dk. \end{aligned} \tag{52}$$

Assuming that the integral length scale for v is much larger than ℓ_v, we may use the inertial subrange expression

$$F_v(k) = \frac{2}{3}\alpha_1\varepsilon^{2/3}k^{-5/3} \tag{53}$$

for the spectrum of v. For later purposes, we assume the values $\alpha_1 k^{4/3} = 0.165$ and $\kappa = 0.4$.

The loss of variance can now be evaluated. The result is

$$\langle v^2\rangle - U^2\langle\phi^2\rangle = \frac{4}{3}\alpha_1(\varepsilon\ell_v)^{2/3}\{h(\zeta) - 2(1-2\zeta^2)g(\zeta)\}, \tag{54}$$

where

$$g(\zeta) = \int_0^{\infty}\frac{s^{1/3}}{(1-s^2)^2 + 4\zeta^2s^2}ds \tag{55}$$

and

$$h(\zeta) = \int_0^\infty \frac{s^{7/3}}{(1-s^2)^2 + 4\zeta^2 s^2} ds. \tag{56}$$

These integrals can be expressed in terms of well-known functions as

$$g(\zeta) = \frac{\pi}{\sqrt{3}} \times \begin{cases} \dfrac{\sin\left(\frac{2}{3}\tan^{-1}(\sqrt{1-\zeta^2}/\zeta)\right)}{2\zeta\sqrt{1-\zeta^2}} & , \quad 0 < \zeta < 1 \\ \frac{1}{3} & , \quad \zeta = 1 \\ \dfrac{\sinh\left(\frac{2}{3}\ln(\zeta + \sqrt{\zeta^2-1})\right)}{2\zeta\sqrt{\zeta^2-1}} & , \quad 1 < \zeta < \infty \end{cases} \tag{57}$$

and

$$h(\zeta) = \frac{\pi}{\sqrt{3}} \times \begin{cases} \dfrac{\sin\left(\frac{4}{3}\tan^{-1}(\sqrt{1-\zeta^2}/\zeta)\right)}{2\zeta\sqrt{1-\zeta^2}} & , \quad 0 < \zeta < 1 \\ \frac{2}{3} & , \quad \zeta = 1 \\ \dfrac{\sinh\left(\frac{4}{3}\ln(\zeta + \sqrt{\zeta^2-1})\right)}{2\zeta\sqrt{\zeta^2-1}} & , \quad 1 < \zeta < \infty \end{cases} \quad , \tag{58}$$

which are shown in Figure 7.

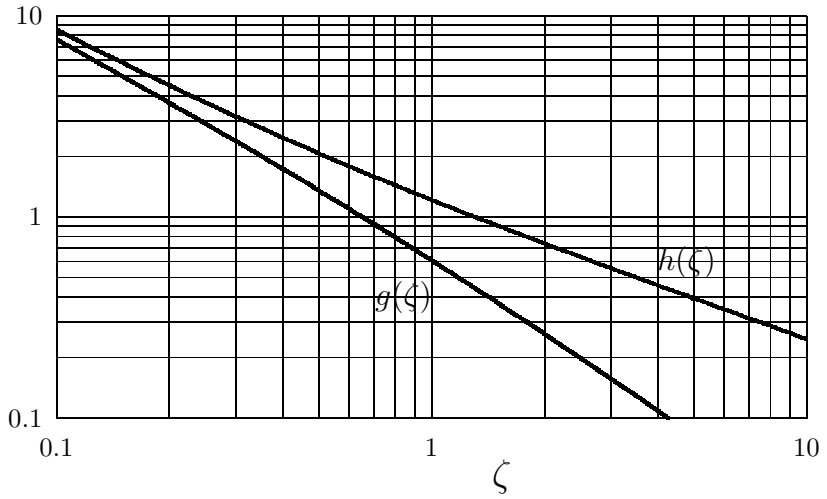

Figure 7. The functions $g(\zeta)$ and $h(\zeta)$ given by (57) and (58), respectively.

Figure 8 displays the function

$$\Delta(\zeta) = h(\zeta) - 2(1-2\zeta^2)g(\zeta). \tag{59}$$

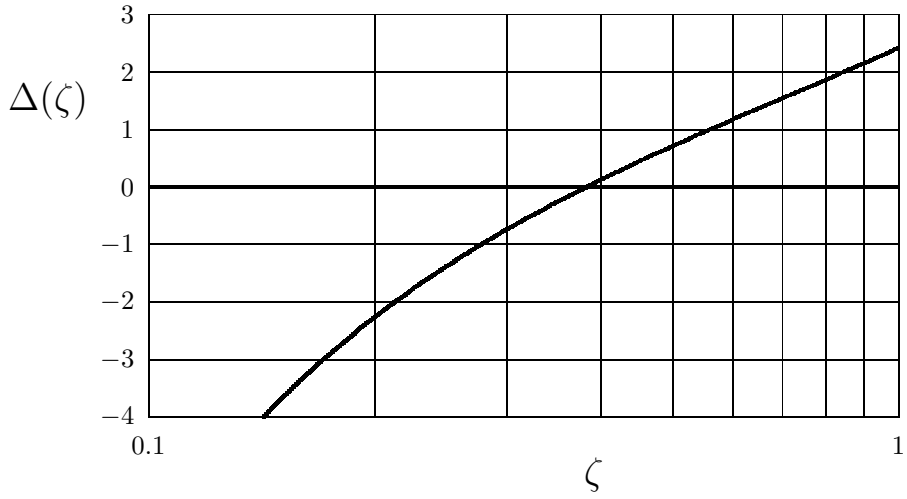

Figure 8. The function $\Delta(\zeta)$ given by (59).

We see that when ζ is smaller than a certain value $\zeta_0 < 1/\sqrt{2}$, then the loss of variance is *negative*, i.e. that the measured variance is too large.

To determine ζ_0 we must solve the equation

$$h(\zeta_0) = 2(1 - 2\zeta_0^2)g(\zeta_0). \tag{60}$$

Using (57) and (58), we obtain, by applying standard operations on trigonometric functions, that this implies that

$$s \tan\left(\frac{1}{3}\tan^{-1}(s)\right) = 1, \tag{61}$$

where

$$s = \frac{\sqrt{1-\zeta_0^2}}{\zeta_0}. \tag{62}$$

After a slight re-arrangement (61) becomes

$$\tan^{-1}(s) - 3\tan^{-1}\left(\frac{1}{s}\right) = 0 \tag{63}$$

or

$$\frac{s - \tan\left(3\tan^{-1}\left(\frac{1}{s}\right)\right)}{1 + s\tan\left(3\tan^{-1}\left(\frac{1}{s}\right)\right)} = 0. \tag{64}$$

Further,

$$\tan(3u) = \frac{3 - \tan^2(u)}{1 - 3\tan^2(u)}, \tag{65}$$

so that (64) implies

$$s^2 - 3 = 3 - s^{-2} \tag{66}$$

with the possible solutions

$$s^2 = 3 \pm \sqrt{8}. \tag{67}$$

Since

$$\zeta_0 = \frac{1}{\sqrt{1 + s^2}}, \tag{68}$$

we must seek ζ_0 among the solutions

$$\zeta_0 = \frac{1}{\sqrt{4 \pm \sqrt{8}}}. \tag{69}$$

We know already that ζ_0 must be smaller than $1/\sqrt{2}$ and the only possibility is then

$$\zeta_0 = \frac{1}{\sqrt{4 + \sqrt{8}}} \approx 0.383, \tag{70}$$

which, by insertion, is easily seen to be a solution.

For neutral stratification we have

$$\langle v^2 \rangle = 2.68 u_*^2 \tag{71}$$

and

$$\varepsilon = \frac{u_*^3}{\kappa z}, \tag{72}$$

so that the *relative* loss of variance becomes

$$\frac{\langle v^2 \rangle - U^2 \langle \phi^2 \rangle}{\langle v^2 \rangle} = 0.513 \times \Delta(\zeta) \times \left(\frac{\ell_v}{z} \right)^{2/3}. \tag{73}$$

$\ell_v = 0.5$ m is a typical value for a fast vane. When $z = 10$ m the loss of variance becomes about -5% for $\zeta = 0.3$ and 17% for $\zeta = 1$.

Figure 9 illustrates the effect of the filtering when $\zeta = \zeta_0$: the area between the two curves to the left of their intersection is equal to the area between the curves to the right of the intersection.

It is very easy to extend the analysis to include spectra which follow a more general power law, i.e.

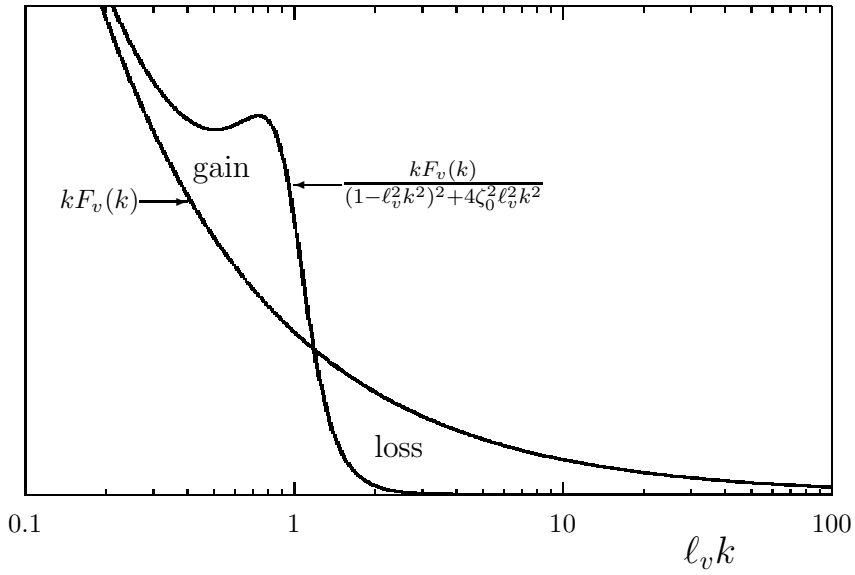

Figure 9. The filtered and unfiltered spectrum of the lateral velocity component in an area conserving representation.

$$F_v(k) = Ak^{-\beta}. \tag{74}$$

If the integral in (52) is convergent, the constant β is limited to the range

$$1 < \beta < 3. \tag{75}$$

The loss of variance is now

$$\begin{aligned} \langle v^2\rangle - U^2\langle\phi^2\rangle &= 2A\ell_v^{\beta-1}\int_0^\infty \frac{s^{4-\beta} - 2(1-2\zeta^2)s^{2-\beta}}{(1-s^2)^2+4\zeta^2s^2}ds \\ &= 2A\ell_v^{\beta-1}\{h_\beta(\zeta) - 2(1-2\zeta^2)g_\beta(\zeta)\} \end{aligned} \tag{76}$$

with

$$\left\{\begin{array}{c} g_\beta(\zeta) \\ h_\beta(\zeta) \end{array}\right\} = \frac{\pi}{4\cos(\beta\frac{\pi}{2})} \times \left\{\begin{array}{c} \frac{\sin((1-\beta)\cos^{-1}(\zeta))}{\zeta\sqrt{1-\zeta^2}} \\ \frac{\sin((\beta-3)\cos^{-1}(\zeta))}{\zeta\sqrt{1-\zeta^2}} \end{array}\right\} \qquad 0<\zeta<1, \tag{77}$$

where we have left out the case of ζ values ≥ 1.

Applying the identity

$$\cos(2\cos^{-1}(\zeta)) = 2\cos^2(\cos^{-1}(\zeta)) - 1 = 2\zeta^2 - 1, \tag{78}$$

we obtain

$$\Delta_\beta(\zeta) = h_\beta(\zeta) - 2(1-2\zeta^2)g_\beta(\zeta) = -\frac{\pi}{4\cos(\beta\frac{\pi}{2})}\frac{\sin((1+\beta)\cos^{-1}(\zeta))}{\zeta\sqrt{1-\zeta^2}}. \tag{79}$$

It is very easy from (79) to determine the value ζ_0 of the damping coefficient for which the variance loss is exactly zero. Since this value is limited to the open interval between zero and one, we get immediately

$$\zeta_0 = \cos\left(\frac{\pi}{\beta+1}\right). \tag{80}$$

We find several special values:

$$\begin{aligned}
\beta = \tfrac{3}{2} &\implies \zeta_0 = \cos\left(\tfrac{2\pi}{5}\right) = \cos(72^\circ) = \frac{\sqrt{5}-1}{4} \approx 0.31 \\
\beta = \tfrac{5}{3} &\implies \zeta_0 = \cos\left(\tfrac{3\pi}{8}\right) = \cos(67.5^\circ) = \frac{1}{\sqrt{4+\sqrt{8}}} \approx 0.38 \\
\beta = 2 &\implies \zeta_0 = \cos\left(\tfrac{\pi}{3}\right) = \cos(60^\circ) = \frac{1}{2} = 0.50
\end{aligned}$$

The filtered and unfiltered spectra are displayed for these three cases in Figures 10, 11 and 12.

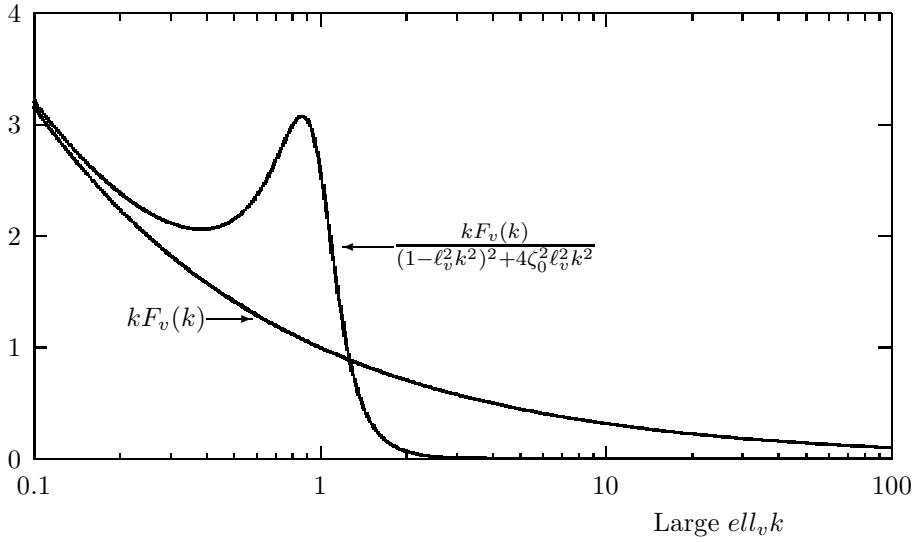

Figure 10. The filtered and unfiltered spectrum of the lateral velocity component in an area conserving representation. $\beta = 3/2$, $\zeta_0 = (\sqrt{5}-1)/4$.

We may quantify the amount of lost variance which is recovered by using a filter with a damping coefficient given by (80). One way is to determine the area between the two curves in e.g. Figure 10 and normalize it by the true variance in the same wave-number interval. This dimensionless number is a function only of β and is given by

$$\begin{aligned}
D(\beta) &= (\beta-1)\left\{2\sin\left(\frac{\pi}{2(\beta+1)}\right)\right\}^{(\beta-1)} \\
&\quad \times \int_{2\sin\left(\frac{\pi}{2(\beta+1)}\right)}^{\infty} \left\{1 - \frac{1}{(1-s^2)^2 + 4\cos^2\left(\frac{\pi}{\beta+1}\right)s^2}\right\} s^{-\beta} ds
\end{aligned} \tag{81}$$

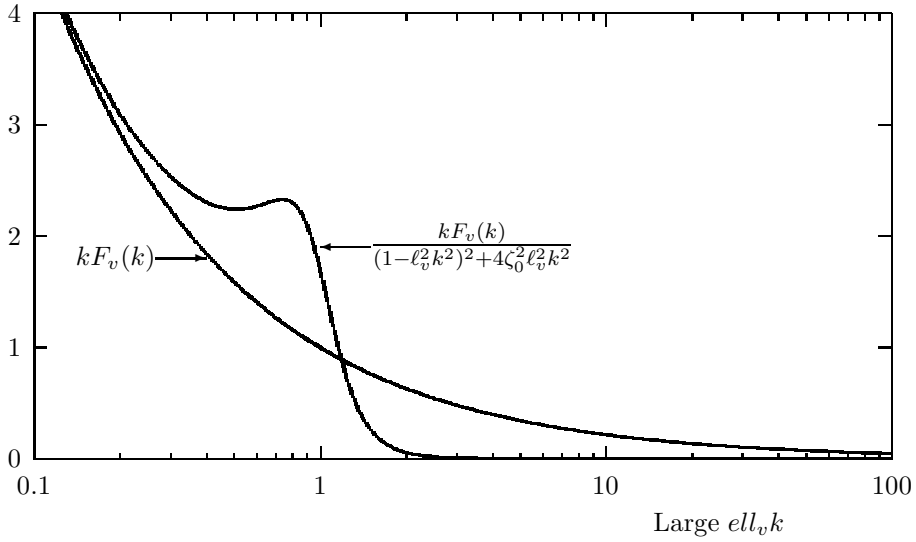

Figure 11. The filtered and unfiltered spectrum of the lateral velocity component in an area conserving representation. $\beta = 5/3$, $\zeta_0 = 1/\sqrt{4+\sqrt{8}}$.

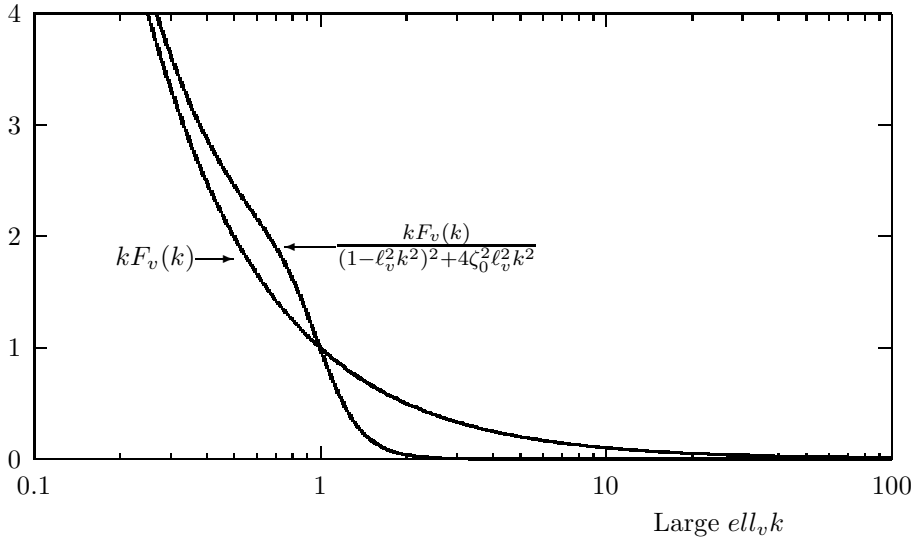

Figure 12. The filtered and unfiltered spectrum of the lateral velocity component in an area conserving representation. $\beta = 2$, $\zeta_0 = 1/2$.

and displayed in Figure 13.

It is easy to evaluate $D(\beta)$ in the limit $\beta \to 1$. We get

$$\lim_{\beta \to 1} D(\beta) = 1, \tag{82}$$

as also indicated by Figure 13.

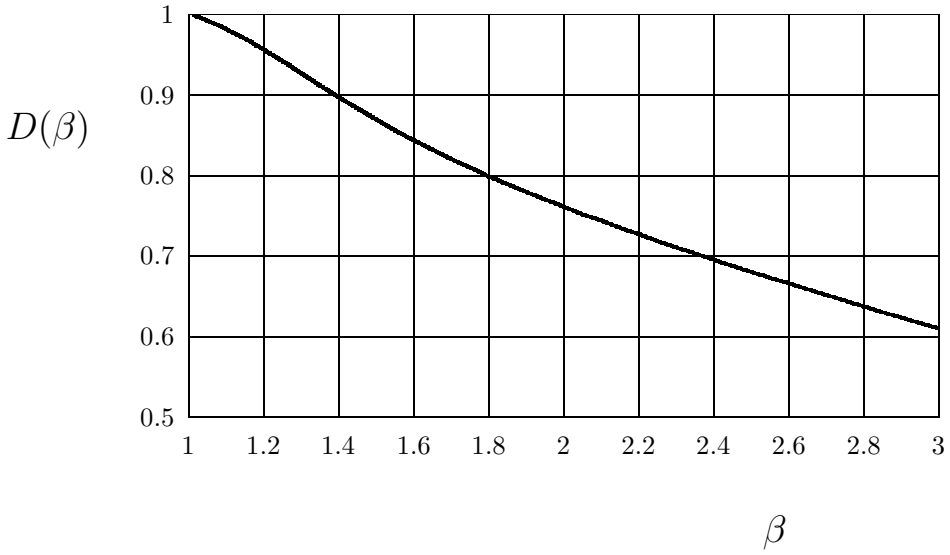

Figure 13. The function $D(\beta)$ given by (81).

5 Cup and Vane

We have seen that the mean wind speed was given by (21). This equation shows that UT is the total distance a hypothetical air particle would travel in the period T if the wind were constant in space (but not necessarily in time). Each revolution of the cup rotor corresponds to the passage through the anemometer of a column of air of length $2\pi\ell$.

However, the average wind-vane direction $\tilde{\phi}_i$ will in general change from one revolution to the next and, if we want to know how far from the starting point our hypothetical air particle has traveled horizontally in the period T, we must add all the small distances $2\pi\ell$ *vectorwise*. This procedure is illustrated in Figure 14. We will redefine the average wind speed as the length of the resulting vector divided by T and wind direction as the direction of this vector. With the x-axis pointing east and the y-axis pointing north, the resulting displacement vector has the two components (UT, VT).

In mathematical terms (U, V) are given by

$$\left\{ \begin{array}{c} U \\ V \end{array} \right\} = \frac{2\pi\ell}{T} \left\{ \begin{array}{c} \sum_{i=1}^{N} \cos(\tilde{\phi}_i) \\ \sum_{i=1}^{N} \sin(\tilde{\phi}_i) \end{array} \right\}. \tag{83}$$

The mean direction $\langle\tilde{\phi}\rangle$ is then computed from the equation

$$\langle\tilde{\phi}\rangle = \arctan\left(\frac{V}{U}\right). \tag{84}$$

The practical way of obtaining the information about both speed and direction is to let each full rotation of a cup anemometer trigger a recording of $\cos(\tilde{\phi})$ and

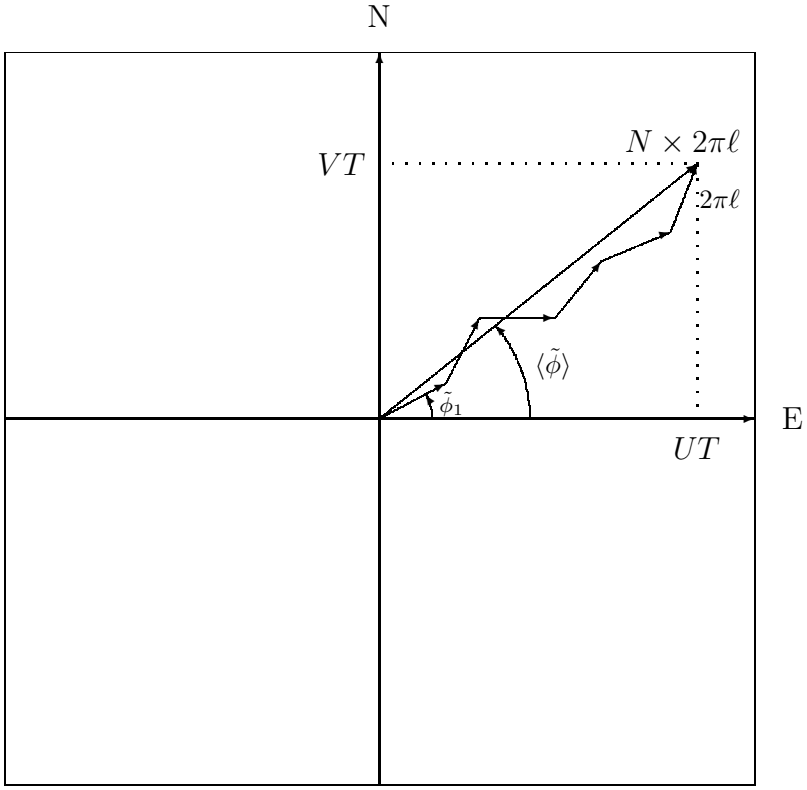

Figure 14. Illustration of the vector wind run.

$\sin(\tilde{\phi})$. It is important in this context that the distance constant of the anemometer ℓ_0 matches the distance constant of the wind vane ℓ_{eff}.

Kristensen (1993) pointed out that, as a bonus, also the (filtered) wind direction variance can be obtained using this type of recording. By expanding $\langle\cos(\phi)\rangle^2$ and $\langle\sin(\phi)\rangle^2$ in the deviation $\delta\phi$ from $\langle\phi\rangle$, a simple analysis shows

$$\langle\delta\phi^2\rangle = 1 - \langle\cos(\phi)\rangle^2 - \langle\sin(\phi)\rangle^2 + \text{ terms of order } \langle\delta\phi^2\rangle^2 \text{ and higher.} \qquad (85)$$

In other words, due to the linearity of the cup anemometer calibration it is possible in a simple way to obtain three mean quantities, wind speed, wind direction and wind-direction variance—quantities important in e.g. dispersion measurements.

6 Prop and Vane

Figure 15 is a schematic diagram of the propeller-vane anemometer.

When the propeller is guided into the wind by means of the vane we realize that the propeller axis cannot be aligned exactly along the mean wind

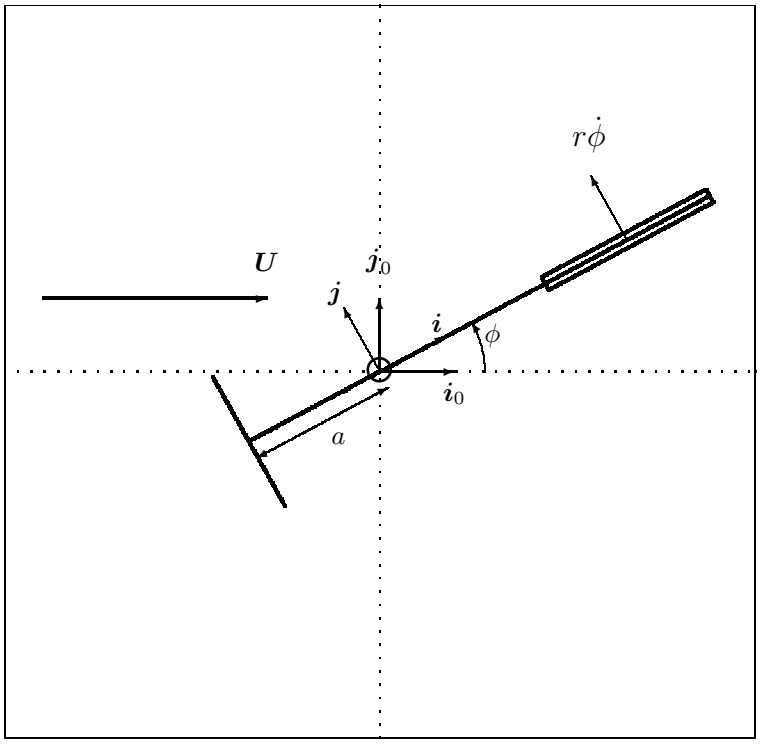

Figure 15. Schematic top view of the propeller-vane geometry and motion.

$$\boldsymbol{U} = \langle \tilde{\boldsymbol{u}} \rangle = \langle \tilde{u} \rangle \, \boldsymbol{i}_0, \tag{86}$$

where

$$\tilde{\boldsymbol{u}} \equiv \tilde{u}\boldsymbol{i}_0 + \tilde{v}\boldsymbol{j}_0 + \tilde{w}\boldsymbol{k}_0 \equiv \tilde{\boldsymbol{h}} + \tilde{w}\boldsymbol{k}_0. \tag{87}$$

The mean wind direction is characterized by the unit vector $\boldsymbol{i}_0$, the lateral and the vertical directions by the unit vectors $\boldsymbol{j}_0$ and $\boldsymbol{k}_0$.

The three components of the instantaneous wind speed are

$$\left\{ \begin{array}{c} \tilde{u} \\ \tilde{v} \\ \tilde{w} \end{array} \right\} = \left\{ \begin{array}{c} U + u \\ v \\ w \end{array} \right\}, \tag{88}$$

where

$$\langle u \rangle = \langle v \rangle = \langle w \rangle = 0. \tag{89}$$

The instantaneous angle from the mean wind direction $\boldsymbol{i}_0$ to the direction of the vane axis $\boldsymbol{i}$ is ϕ. The center of the propeller has the distance a from the vane axis so that the position of this center is $-a\cos(\phi)\,\boldsymbol{i}_0 - a\sin(\phi)\,\boldsymbol{j}_0$. Consequently, the velocity of the propeller center becomes

$$\boldsymbol{v}_{\mathrm{p}} = \frac{d}{dt}\left\{-a\cos(\phi)\,\boldsymbol{i}_0 - a\sin(\phi)\,\boldsymbol{j}_0\right\} = a\dot{\phi}\sin(\phi)\,\boldsymbol{i}_0 - a\dot{\phi}\cos(\phi)\,\boldsymbol{j}_0. \tag{90}$$

The instantaneous wind velocity, experienced by the propeller in the moving reference frame of the vane, is therefore

$$\tilde{\boldsymbol{u}} - \boldsymbol{v}_{\mathrm{p}} = \{U + u - a\dot{\phi}\sin\phi\}\,\boldsymbol{i}_0 + \{v + a\dot{\phi}\cos\phi\}\,\boldsymbol{j}_0 + w\,\boldsymbol{k}_0. \tag{91}$$

The relation between the coordinate system $\boldsymbol{i}_0, \boldsymbol{j}_0$, $\boldsymbol{k}_0$, determined by the mean wind vector, and the coordinate system of the vane $\boldsymbol{i}$, $\boldsymbol{j}$, $\boldsymbol{k}$ is

$$\left\{\begin{array}{c}\boldsymbol{i}_0\\ \boldsymbol{j}_0\\ \boldsymbol{k}_0\end{array}\right\} = \left\{\begin{array}{ccc}\cos(\phi) & -\sin(\phi) & 0\\ \sin(\phi) & \cos(\phi) & 0\\ 0 & 0 & 1\end{array}\right\}\left\{\begin{array}{c}\boldsymbol{i}\\ \boldsymbol{j}\\ \boldsymbol{k}\end{array}\right\}, \tag{92}$$

so that the relative velocity $\tilde{\boldsymbol{u}} - \boldsymbol{v}_{\mathrm{p}}$ in the propeller coordinate system becomes

$$\begin{aligned}\tilde{\boldsymbol{u}} - \boldsymbol{v}_{\mathrm{p}} &= \{U + u - a\dot{\phi}\sin(\phi)\}\{\cos(\phi)\,\boldsymbol{i} - \sin(\phi)\,\boldsymbol{j}\}\\ &\quad + \{v + a\dot{\phi}\cos(\phi)\}\{\sin(\phi)\,\boldsymbol{i} + \cos(\phi)\,\boldsymbol{j}\} + w\,\boldsymbol{k}\\ &= \{U\cos(\phi) + u\cos(\phi) + v\sin(\phi)\}\,\boldsymbol{i}\\ &\quad - \{U\sin(\phi) + u\sin(\phi) - v\cos(\phi) - a\dot{\phi}\}\,\boldsymbol{j} + w\,\boldsymbol{k}.\end{aligned} \tag{93}$$

We assume that $\phi \ll 1$ and that the numerical values of u, v and w are much smaller than U. Further, we assume that $a|\dot{\phi}| \ll U$ and expand (93) to second order in the small quantities. The result is

$$\begin{aligned}\tilde{\boldsymbol{u}} - \boldsymbol{v}_{\mathrm{p}} &\approx U\,\boldsymbol{i} + u\,\boldsymbol{i} + \{v + a\dot{\phi} - U\phi\}\,\boldsymbol{j} + w\,\boldsymbol{k}\\ &\quad + \{v\phi - \frac{U}{2}\phi^2\}\,\boldsymbol{i} - u\phi\,\boldsymbol{j}.\end{aligned} \tag{94}$$

We substitute (94) and

$$\tilde{s} = S + s \tag{95}$$

in (29) and, using the expression (30), we obtain to second order

$$\begin{aligned}\frac{\ell_0}{U}\dot{s} + s &\approx \frac{u}{\ell} + \frac{us - \ell s^2}{U}\\ &\quad + \frac{v\phi - \frac{1}{2}U\phi^2}{\ell} + \mu_2\frac{\{v + a\dot{\phi} - U\phi\}^2 + w^2}{2\ell U}.\end{aligned} \tag{96}$$

Equation (96) is a first-order ordinary differential equation in s. The right-hand side contains first and second-order terms. The known variables are u, v and w. The fourth variable ϕ is determined by the dynamic equation (50) for the vane.

We have defined the velocity variables such that they fulfil (89). Equation (50) implies that also

$$\langle \phi \rangle = 0. \tag{97}$$

However, the way s is defined by (95) does not guarantee the mean of s is zero. In fact, taking the average of (96), we get

$$\begin{aligned} \langle s \rangle \quad &= \quad \frac{1}{U}\{\langle us \rangle - \ell \langle s^2 \rangle\} \\ &\quad + \frac{1}{\ell}\{\langle v\phi \rangle - \frac{U}{2}\langle \phi^2 \rangle\} + \frac{\mu_2}{2\ell U}\{\langle (v + a\dot{\phi} - U\phi)^2 \rangle + \langle w^2 \rangle\}. \end{aligned} \tag{98}$$

In order to determine $\langle s \rangle$, we must evaluate all the second-order terms on the right-hand side of (98). The terms involving s are zero in our approximation since s to the first order fulfills the differential equation

$$\frac{\ell_0}{U}\dot{s} + s = \frac{u}{\ell}. \tag{99}$$

Multiplying this equation on both sides by s and averaging yield

$$\langle s^2 \rangle = \langle us \rangle / \ell, \tag{100}$$

which shows that the two first term on the right-hand side of (98) cancel.

In order to determine the other terms we must solve (50) with the initial conditions $\phi(-\infty) = 0$ and $\dot{\phi}(-\infty) = 0$. The result is

$$\phi(t) = \frac{\omega_0}{\sqrt{1-\zeta^2}} \frac{1}{U} \int_0^\infty v(t-\tau) \mathrm{e}^{-\zeta\omega_0\tau} \sin(\sqrt{1-\zeta^2}\omega_0\tau) d\tau. \tag{101}$$

We obtain immediately

$$\langle \phi^2 \rangle = \frac{1}{U^2} \int_{-\infty}^{\infty} \frac{\omega_0^4 S_v(\omega)}{(\omega_0^2 - \omega^2)^2 + 4\zeta^2\omega_0^2\omega^2} d\omega \tag{102}$$

and

$$\langle v\phi \rangle = \frac{1}{U} \int_{-\infty}^{\infty} \frac{\omega_0^2(\omega_0^2 - \omega^2) S_v(\omega)}{(\omega_0^2 - \omega^2)^2 + 4\zeta^2\omega_0^2\omega^2} d\omega, \tag{103}$$

where $S_v(\omega)$ is the power spectrum of v.

Multiplying (50) by either ϕ or by $\dot{\phi}$, followed by averaging, we easily obtain the two relations

$$-\langle \dot{\phi}^2 \rangle + \omega_0^2 \langle \phi^2 \rangle = \omega_0^2 \frac{\langle v\phi \rangle}{U} \tag{104}$$

and

$$2\zeta\omega_0\langle\dot{\phi}^2\rangle = \omega_0^2\frac{\langle v\dot{\phi}\rangle}{U}, \tag{105}$$

so that

$$\frac{\langle\dot{\phi}^2\rangle}{\omega_0^2} = \frac{\langle v\dot{\phi}\rangle}{2\zeta\omega_0 U} = \langle\phi^2\rangle - \frac{\langle v\phi\rangle}{U}. \tag{106}$$

With (106) we can now evaluate the relative bias $\delta = \langle s\rangle/S$ in terms of $\langle\phi^2\rangle$ and $\langle v\phi\rangle/U$:

$$\begin{aligned}\delta &= (1-\mu_2)\left(\frac{\langle v\phi\rangle}{U} - \frac{\langle\phi^2\rangle}{2}\right)\\ &\quad + \mu_2\left\{\frac{\langle v^2\rangle + \langle w^2\rangle}{2U^2} + \left(\frac{a^2\omega_0^2}{2U^2} + 2\zeta\frac{a\omega_0}{U}\right)\left(\langle\phi^2\rangle - \frac{\langle v\phi\rangle}{U}\right)\right\}.\end{aligned} \tag{107}$$

Using (102) and (103), we get

$$\begin{aligned}\delta &= \frac{\langle v^2\rangle + \mu_2\langle w^2\rangle}{2U^2}\\ &\quad - \frac{1-\mu_2}{2U^2}\int_{-\infty}^{\infty}\frac{\omega^2(\omega^2 + 4\zeta^2\omega_0^2)S_v(\omega)}{(\omega_0^2-\omega^2)^2 + 4\zeta^2\omega_0^2\omega^2}d\omega\\ &\quad + \frac{\mu_2}{2U^2}\left(\frac{a^2\omega_0^2}{U^2} + 4\zeta\frac{a\omega_0}{U}\right)\int_{-\infty}^{\infty}\frac{\omega_0^2\omega^2 S_v(\omega)}{(\omega_0^2-\omega^2)^2 + 4\zeta^2\omega_0^2\omega^2}d\omega.\end{aligned} \tag{108}$$

Introducing the vane distance constant ℓ_v and applying, once again, Taylor's hypothesis, we can write (108) in the form

$$\begin{aligned}\delta &= \frac{\langle v^2\rangle + \mu_2\langle w^2\rangle}{2U^2}\\ &\quad - \frac{1-\mu_2}{2U^2}\int_{-\infty}^{\infty}\frac{k^2\ell_v^2(k^2\ell_v^2 + 4\zeta^2)F_v(k)}{(1-k^2\ell_v^2)^2 + 4\zeta^2k^2\ell_v^2}dk\\ &\quad + \frac{\mu_2}{2U^2}\left(\frac{a^2}{\ell_v^2} + 4\zeta\frac{a}{\ell_v}\right)\int_{-\infty}^{\infty}\frac{k^2\ell_v^2F_v(k)}{(1-k^2\ell_v^2)^2 + 4\zeta^2k^2\ell_v^2}dk.\end{aligned} \tag{109}$$

Assuming that ℓ_v is much smaller than the integral scale of $v(t)$, we may use (53) for $F_v(k)$.

This leads to the expression

$$\begin{aligned}\delta &= \frac{\langle v^2\rangle + \mu_2\langle w^2\rangle}{2U^2}\\ &\quad - \frac{1-\mu_2}{2U^2}\frac{4}{3}\alpha_1(\varepsilon\ell_v)^{2/3}\{4\zeta^2g(\zeta) + h(\zeta)\}\\ &\quad + \frac{\mu_2}{2U^2}\left\{\frac{a^2}{\ell_v^2} + 4\zeta\frac{a}{\ell_v}\right\}\frac{4}{3}\alpha_1(\varepsilon\ell_v)^{2/3}g(\zeta),\end{aligned} \tag{110}$$

where $g(\zeta)$ and $h(\zeta)$ are given by (57) and (58).

In the neutrally stratified surface layer we have (e.g. see Kristensen *et al.* (1989))

$$\langle v^2 \rangle = 2.68\, u_*^2, \tag{111}$$

$$\langle w^2 \rangle = 1.46\, u_*^2 \tag{112}$$

and, assuming local balance between shear production and destruction by dissipation of turbulent kinetic energy,

$$\varepsilon = \frac{u_*^3}{\kappa z}. \tag{113}$$

Using the same values as Kristensen *et al.* (1989) with $\alpha_1 \kappa^{4/3} = 0.165$ and $\kappa = 0.4$, we can write (110) in the form

$$\begin{aligned} \frac{\delta}{\langle v^2 \rangle / (2U^2)} \quad = \quad & 1 + 0.54\mu_2 \\ & - 0.51(1-\mu_2)\{4\zeta^2 g(\zeta) + h(\zeta)\} \left(\frac{\ell_v}{z}\right)^{2/3} \\ & + 0.51\mu_2 \left\{ \frac{a^2}{\ell_v^2} + 4\zeta \frac{a}{\ell_v} \right\} g(\zeta) \left(\frac{\ell_v}{z}\right)^{2/3}. \end{aligned} \tag{114}$$

As an example, let us apply (114) to the Gill propeller vane type 35003D. According to Monna (1978) and Monna and Driedonks (1979), this model has $a \approx 0.35$ m, $\ell_v \approx 1.0$ m and $\zeta \approx 0.6$. Further, Monna and Driedonks (1979) found that the angular response of the Gill propeller can be written

$$\mathcal{G}(\vartheta) = \cos(1.3\vartheta) \approx \cos(\vartheta) - 0.35\vartheta^2, \tag{115}$$

which, by comparison with (31), shows that $\mu_2 \approx -0.7$.

Inserting in (114) we obtain

$$\frac{\delta}{\langle v^2 \rangle / (2U^2)} = 0.62 - 3.3 \left(\frac{\ell_v}{z}\right)^{2/3} \tag{116}$$

for this Gill propeller vane.

A general comparison between the propeller vane and a cup vane is most easily carried out by going back to (110). The two first terms in this equation are the same as those we found for the cup anemometer (Kristensen, 1993). They are the v-bias and the w-bias, respectively. The rest of the propeller-vane bias in (110) we denote $\delta_{\rm pv}$. This bias occurs partly because the vane is lagging behind the instantaneous wind direction and partly because the vane itself moves with respect to the wind. We see that the two terms in $\delta_{\rm pv}$ have a common dimensionless factor, namely

$$B = \frac{2}{3}\alpha_1 \frac{(\varepsilon \ell_v)^{2/3}}{U^2}. \tag{117}$$

In the horizontally homogeneous, diabatic surface layer both U and ε are stability dependent so in general B is also stability dependent.

Following e.g. Panofsky and Dutton (1984), we have

$$\varepsilon = \frac{u_*^3}{\kappa z}\varphi_\varepsilon\Big(\frac{z}{L}\Big) \tag{118}$$

and

$$U = \frac{u_*}{\kappa}\left\{\ln\Big(\frac{z}{z_0}\Big) - \psi_m\Big(\frac{z}{L}\Big)\right\}, \tag{119}$$

where L is the Monin-Obukhov length and z_0 the roughness length.

The two functions $\varphi_\varepsilon(z/L)$ and $\psi_m(z/L)$ are

$$\varphi_\varepsilon\Big(\frac{z}{L}\Big) = \varphi_m\Big(\frac{z}{L}\Big) - \frac{z}{L} \tag{120}$$

and

$$\psi_m\Big(\frac{z}{L}\Big) = \int_{z_0/L}^{z/L}[1-\varphi_m(s)]\frac{ds}{s} \approx \int_0^{z/L}[1-\varphi_m(s)]\frac{ds}{s}, \tag{121}$$

where

$$\varphi_m\Big(\frac{z}{L}\Big) \equiv \frac{\kappa z}{u_*}\frac{dU}{dz}. \tag{122}$$

According to Panofsky and Dutton (1984) we have

$$\varphi_m(s) = \begin{cases} (1-16s)^{-1/3} & , \quad s \le 0 \\ \\ 1+5s & , \quad s > 0 \end{cases}, \tag{123}$$

so that for $z/L \le 0$

$$\psi_m\Big(\frac{z}{L}\Big) = \frac{3}{2}\ln\Big(\frac{1+\xi+\xi^2}{3}\Big) - \sqrt{3}\tan^{-1}\Big(\frac{1}{\sqrt{3}}\frac{\xi-1}{\xi+1}\Big) \tag{124}$$

with $\xi = 1/\varphi_m(z/L)$, while for $z/L > 0$

$$\psi_m\Big(\frac{z}{L}\Big) = -5\frac{z}{L}. \tag{125}$$

We can now write

$$B = \chi_{\rm pv}\Big(\frac{z}{z_0}, \frac{z}{L}\Big) \times \Big(\frac{\ell_v}{z}\Big)^{2/3}, \tag{126}$$

where

$$\chi_{\rm pv}\left(\frac{z}{z_0},\frac{z}{L}\right)=\frac{2}{3}\phi_1\kappa^{4/3}\left\{\ln\left(\frac{z}{z_0}\right)-\psi_m\left(\frac{z}{L}\right)\right\}^{-2}\varphi_\varepsilon^{2/3}\left(\frac{z}{L}\right). \qquad (127)$$

Finally, we obtain

$$\begin{aligned}\delta_{\rm pv} &= -\left\{(1-\mu_2)(4\zeta^2 g(\zeta)+h(\zeta))-\mu_2\left(\frac{a^2}{\ell_v^2}+4\zeta\frac{a}{\ell_v}\right)g(\zeta)\right\}\\ &\quad\times\chi_{\rm pv}\left(\frac{z}{z_0},\frac{z}{L}\right)\times\left(\frac{\ell_v}{z}\right)^{2/3}. \qquad (128)\end{aligned}$$

The function $\chi_{\rm pv}(z/z_0, z/L)$ is displayed in Fig. 16 for two typical values of z/z_0.

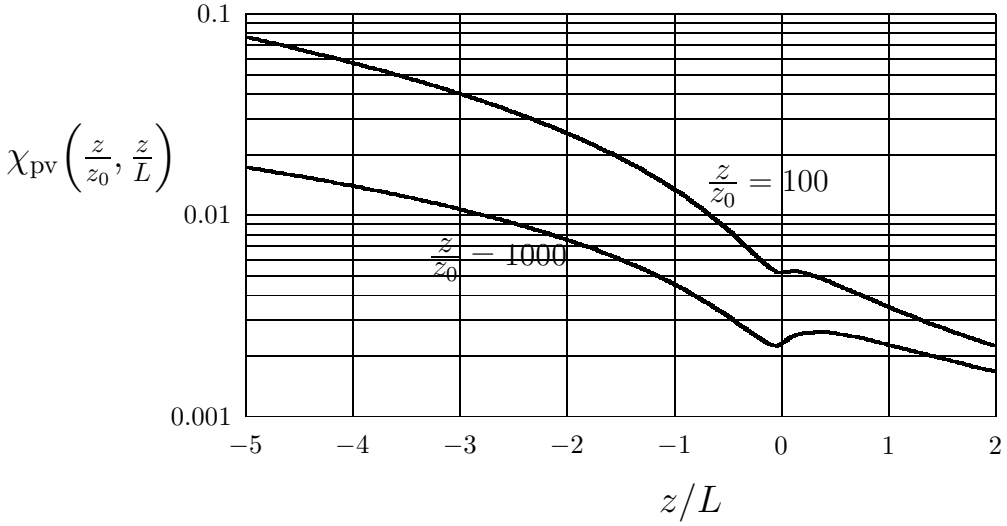

Figure 16. The function $\chi_{\rm pv}(z/z_0, z/L)$ as given by (127).

7 Conclusions

This report has been inspired by a number of unanswered questions which arose during and after the writing of the report by Kristensen (1993). Consequently, it has not been possible to keep as well a logical order in dealing with these questions. Two of the errors which have later been found in Kristensen (1993) are reported here in footnotes.

Concerning the cup anemometer, the question of overspeeding was discussed in much detail by Kristensen (1993) so we have only restated, in section 2 the phenomenological model for the forcing of the cup rotor and pointed out that there is no inconsistencies between this model and the experimental findings by Wyngaard *et al.* (1974) and Coppin (1982). Further is pointed out in subsection 2.3 that simple determination of the mean-wind speed in a sense is ambiguous since a calculation of the time average $\widehat{U}$ of the mean-wind speeds in each revolution of

the cup rotor is systematically larger than the mean wind speed U calculated by counting the number of rotor revolutions during the averaging period. The overestimation is approximately proportional to the ratio of variance of the mean wind speeds in each revolution and U^2 and thus more important the more turbulent the wind.

In section 3 we apply the same type of phenomenological model to the forcing of the propeller. In a way this model is simpler than that for the cup anemometer since it requires only three parameters, the calibration distance ℓ, the distance constant ℓ_0 for a flow along the propeller axis, and a dimensionless parameter μ_2 specifying the symmetric angular response. The corresponding model for the cup anemometer has two more parameters, namely one Λ of dimension length and a dimensionless parameter μ_1 specifying the asymmetric part of the angular response. There has been no experimental verification of the model for the propeller model.

Section 4 is devoted entirely to the wind vane. The equation of motion which is derived according to Larsen and Busch (1974) is, in contrast to the first-order differential equations for the cup and for the propeller, of second-order. Therefore the filter characteristics must be described not only by a distance constant ℓ_v, but also by a damping coefficient ζ. When operated together with a cup or propeller anemometer, it is important to match the distance constants and try to design the vane such that the vane is so overdamped that it approximates a first-order filter. It is argued that, since ζ for sufficiently light vane material is only a function of the vane area and the mass per unit length of the vane arm, it should be possible to match the characteristics of a cup anemometer. This remains to be shown experimentally. In subsection 4.2 we take another approach and show that an underdamped wind vane can be used to determine the wind direction variance without loss. It turns out that if ℓ_v is much smaller than the scale of the turbulence then—theoretically—the high-frequency loss of measured variance can be compensated by the 'overshooting', at lower frequencies, of the underdamped vane. This compensation balances the loss almost exactly if $\zeta = \cos(3\pi/8) = 1/\sqrt{4+\sqrt{8}} \approx 0.38$. It would be very interesting if this could be verified experimentally as it would be useful to measure the lateral variance of the turbulent wind in e.g. studies of turbulent atmospheric dispersion. Actually, it should be easier to construct an underdamped than an overdamped wind vane.

In section 5 we restate an important result from Kristensen (1993). We show that the calibration (4), i.e. $S = U/\ell$, where the calibration ℓ is an instrument constant, suggests that the best way to obtain the mean wind magnitude and direction is to measure, from each revolution of the cup rotor, sine and cosine of the wind direction and average both of these quantities over the averaging time T. In this way we obtain a magnitude which is equal to the so-called wind way, or vector wind run, divided by T (see Figure 14) and, at the same time get an estimate of the wind-direction variance.

Finally, in section 6 we discuss the propeller-vane anemometer. The main question here is whether this instrument has systematic errors like those of the cup anemometer (Kristensen, 1993). It turns out that what is called v-bias and w-bias of a cup anemometer is of exactly the same form for a propeller-vane anemometer. In addition, there are two other sources of bias on the mean-wind speed. The first can be understood qualitatively by noting that the propeller is always lacking behind and will never has its axis aligned with the instantaneous horizontal wind component. Since the wind forcing on the propeller is always, for a given magnitude of the speed, at maximum when the wind is directed along the propeller axis, the rotation rate will always be systematically too small. Therefore this bias contribution is negative. The other source can also be interpreted qualitatively: The

vane is rotating in the horizontal plane around a vertical axis and is displaced the distance a with respect to this axis (see Figure 15). Therefore the propeller has its own motion with respect to the air and, even if the wind speed were exactly zero, the propeller would turn if the vane were turning. The sign of this bias depends on the angular-response parameter μ_2 and the ratio of a to the distance constant ℓ_v of the vane. We note that the propeller distance constant ℓ_0, with the model postulated here, does not have any influence on the bias.

References

Batchelor, G.K. (1967). *An Introduction to Fluid Dynamics*, Cambridge University Press, 615 pp.

Brazier, C.E. (1914). Recherches expérimentales sur les moulenets anémometrique. *Ann. Bur. Centr. Météorol. France*, 157-300; Thèse Fac. Sc. Univ. Paris (1921), ed. Gaurthier-Villars.

Busch, N.E., Christensen, O., Kristensen, L., Lading, L. and Larsen, S.E. (1980). Cups, Vanes, Propellers and Laser Anemometers, *Air-Sea Interaction — Instruments and Methods.*, F. Dobson, L. Hasse and R. Davis, Eds., Plenum Press, NY, 11-46.

Coppin, P.A. (1982). An Examination of Cup Anemometer Overspeeding. *Meteorol. Rdsch.*, **35**, 1-11.

Kristensen, L., Lenschow, D.H., Kirkegaard, P. and Courtney, M.S. (1989). The Spectral Velocity Tensor for Homogeneous Boundary-Layer Turbulence, *Boundary-Layer Meteorol.*, **47**, 149-193.

Kristensen, L. (1993). *The Cup Anemometer and Other Exciting Instruments*, Risø-R-615(EN), Risø National Laboratory, Roskilde, 83 pp.

Larsen, S.E. and Busch, N.E. (1974). Hot-wire Measurements in the Atmosphere. Part I: Calibration and Response Characteristics. *DISA Information*, **16**, 15-34.

Larsen, S.E. (1986). *Hot-wire Measurements of Atmospheric Turbulence Near the Ground*, Risø-R-233, Risø National Laboratory, Roskilde, 342 pp.

Middleton, W.E.K. (1969). *Invention of the Meteorological Instruments*, The Johns Hopkins Press, Baltimore, MD, 362 pp

Monna, W.A.A. (1978). *Comparative Investigation of Dynamic Properties of some Propeller Vanes*, W.R. 78-11, K.N.M.I., de Bilt, the Netherlands, 30 pp.

Monna, W.A.A. and Driedonks, A.G.M. (1979). Experimental Data on the Dynamic Properties of Several Propeller Vanes, *J. Appl. Meteor.*, **18**, 699-702.

Panofsky, H.A. and Dutton, J.A. (1984). *Atmospheric Turbulence*, John Wiley & Sons, NY, 397 pp.

Patterson, J. (1926). The Cup Anemometer. *Trans. Roy. Soc. Canada*, Ser. III, **20**, 1-54.

Wyngaard, J.C., Bauman, J.T. and Lynch, R.A. (1974). Cup Anemometer Dynamics. *Proc. Instrument Society of America*, Pittsburgh, PA, May 10-14, 1971, **1**, 701-708.

Wyngaard, J.C. (1981). Cup, Propeller, Vane, and Sonic Anemometers in Turbulence Research. *Annu. Rev. Fluid Mech.*, **13**, 399-423.

Bibliographic Data Sheet **Risø–R–766(EN)**

Title and author(s)

Cups, Props and Vanes

Leif Kristensen

ISBN	ISSN
87–550–2006–2	0106–2840

Dept. or group	Date
Meteorology and Wind Energy	August 1994

Groups own reg. number(s)	Project/contract No.

Pages	Tables	Illustrations	References
37	1	16	15

Abstract (Max. 2000 char.)

We discuss the dynamics of the cup anemometer, the propeller anemometer and the wind vane. The phenomenological model by Kristensen (1993) is modified to describe the motion of the propeller anemometer. We use the well-know second-order differential equation describing the motion of the wind vane to study the properties of the vane itself and the vane in combination with a cup and a vane. It is argued that even the simplest question about how to record the signal from a cup anemometer has an ambiguous answer and can lead to a, not necessarily small, systematic error in the measured mean wind speed. We show how it is possible to measure the entire wind direction variance by utilizing the fact that an underdamped vane by 'overshooting' may compensate for the high-frequency variance loss if the damping coefficient is about 0.4. Finally we discuss possible sources of bias on the measured mean-wind speed when using a propeller-vane anemometer. It turns out that this anemometer has the same type biases from the lateral and vertical wind fluctuations as has the cup anemometer. In addition there are bias contributions from misalignment between the mean wind and the propeller axis and from the translatory motion of the propeller itself with respect to the vertical wind-vane axis.

Descriptors INIS/EDB

ANEMOMETER; DYNAMICS; FLUCTUATIONS; TURBULENCE; VANES; VELOCITY; WIND

Available on request from Information Service Department, Risø National Laboratory (Afdelingen for Informationsservice, Forskningscenter Risø), P.O. Box 49, DK–4000 Roskilde, Denmark.
Phone +45 46 77 40 04, Fax +45 46 77 40 13, E-mail infserv@risoe.dk